

The performance of chest CT in evaluating the clinical severity of COVID-19 pneumonia: identifying critical cases based on CT characteristics

Peijie Lyu, MD¹, Xing Liu, MS¹, Rui Zhang, MD¹, Lei Shi, MS², Jianbo Gao, MD¹

¹The Department of Radiology, The First Affiliated Hospital of Zhengzhou University; No.1, East Jianshe Road, Zhengzhou, Henan Province, China. Zip Code: 450052.

²CT Collaboration, Siemens Healthineers Ltd

Peijie Lyu and Xing Liu contributed equally to the article.

Corresponding author:

Name: Jianbo Gao

Mailing address: Department of Radiology; The First Affiliated Hospital of Zhengzhou University; No.1, East Jianshe Road, Zhengzhou, Henan Province, China. Postal number 450052.

Phone number: +86-0371-66913114-6809

Fax number: +86-0371-66970906

E-mail address: gjbfsk@126.com

This article is made available via the PMC Open Access Subset for unrestricted re-use and analyses in any form or by any means with acknowledgement of the original source. These permissions are granted for the duration of the COVID-19 pandemic or until permissions are revoked in writing. Upon expiration of these permissions, PMC is granted a perpetual license to make this article available via PMC and Europe PMC, consistent with existing copyright protections.

ACCEPTED

Objectives: To assess the clinical severity of COVID-19 pneumonia using qualitative and/or quantitative chest CT indicators and identify the CT characteristics of critical cases.

Materials and Methods: Fifty-one patients with COVID-19 pneumonia including ordinary cases (group A, n=12), severe cases (group B, n=15) and critical cases (group C, n=24) were retrospectively enrolled. The qualitative and quantitative indicators from chest CT were recorded and compared using Fisher's exact test, one-way ANOVA, Kruskal-Wallis H test and receiver operating characteristic analysis.

Results: Depending on the severity of the disease, the number of involved lung segments and lobes, the frequencies of consolidation, crazy-paving pattern and air bronchogram increased in more severe cases. Qualitative indicators including total severity score for the whole lung and total score for crazy-paving and consolidation could distinguish groups B and C from A (69% sensitivity, 83% specificity and 73% accuracy) but were similar between group B and group C. Combined qualitative and quantitative indicators could distinguish these three groups with high sensitivity (B+C vs. A, 90%; C vs. B, 92%), specificity (100%, 87%) and accuracy (92%, 90%). Critical cases had higher total severity score (>10) and higher total score for crazy-paving and consolidation (>4) than ordinary cases, and had higher mean lung density (>-779HU) and full width at half maximum (>128HU) but lower relative volume of normal lung density ($\leq 50\%$) than ordinary/severe cases. In our critical cases, eight patients with relative volume of normal lung density smaller than 40% received mechanical ventilation for supportive treatment, and two of them had died.

Conclusion: A rapid, accurate severity assessment of COVID-19 pneumonia based on chest CT would be feasible and could provide help for making management decisions, especially for the critical cases.

Keywords: COVID-19, SARS-CoV-2, Quantitative chest CT, Computed Tomography, Viral pneumonia

Abbreviations

COVID-19= coronavirus disease 2019

SARS-CoV-2 = severe acute respiratory syndrome coronavirus 2

ARDS= acute respiratory distress syndrome

Rel.vol= relative volume

MLD= mean lung density

FWHM= full width at half maximum

LAV= low attenuation value

HAV= high attenuation value

Introduction

The outbreak of the coronavirus disease 2019(COVID-19) has spread rapidly throughout Wuhan (Hubei province) to other provinces in China and other more than 75 countries around the world¹⁻⁴, representing a significant and urgent threat to the global health. Severe acute respiratory syndrome coronavirus 2 (SARS-CoV-2), a new virus responsible for the outbreak of respiratory illness known as COVID-19, has sickened more than 95,000 people and killed more than 3,200, most in China, as of Mar 5th, 2020. The clinical spectrum of COVID-19 pneumonia ranges from mild to critical cases, among which the diagnosis of ordinary, severe and critical cases were all correlated with chest CT findings^{5,6}. Previously published studies have described the general typical and atypical CT image manifestations^{6,7}, the time-course evolution of CT findings^{8,9}, the correlation between CT features and clinical features^{1,10}, and evaluated the CT severity of patients with COVID pneumonia^{8,11-17}. In order to reduce or eliminate the subjectivity in the qualitative and semi-quantitative visual evaluation of CT severity scores^{8,15,17}, quantitative approaches for assessing lung opacification percentage of the whole lung have developed, such as deep learning method¹⁸, computer tool¹⁶ or the calculation method of combing mean attenuation values and opacity volumes¹⁴. However, these quantitative analysis methods did not fully specify information characterizing and quantifying different clinical stages with CT features, especially for critical cases.

The rapid and accurate assessment of clinical severity for COVID-19 pneumonia is crucial for early management, treatment, and disease monitoring. Especially for critical cases, early identifications are of paramount importance to reduce mortality. In this study, we aimed to investigate whether the qualitative and/or quantitative indicators from chest CT could identify patients in different clinical stages and further identify the CT characteristics of critical cases.

Materials and Methods:

Given the retrospective nature of this study, written informed consent from all patients was waived by the institutional review board of the Blinded. One author of the study (Blinded) is an employee of CT Collaboration from Siemens Healthineers. The other authors who are not employees of or consultants for any industry had control of all data.

Study design and participates

Clinical electronic medical records and radiological examinations for all patients with laboratory-confirmed SARS-CoV-2 infection from Jan 15, 2019, to Feb 24, 2020, were reviewed. In our hospital, CT scans were routinely performed in symptomatic patients with suspected with COVID-19 disease, defined as those¹⁹ who had exposure history (exposed to infected individuals or epidemic areas) and clinical symptoms (such as fever and cough, etc). Patients who had been diagnosed with COVID-19 pneumonia and received chest CT scans were included in our study. According to the clinical stages of COVID-19 issued by China and WHO interim guidance^{1,20}, patients were assigned to three groups: group A, ordinary cases; group B, severe cases; group C, critical cases. Ordinary cases are defined as those who had clinical symptoms of fever and respiratory tract and positive CT findings of pneumonia. Severe cases are defined as those who had a respiratory rate ≥ 30 times per minute, or oxygen saturation $\leq 93\%$ at rest, or arterial oxygen partial pressure(PaO₂)/inspired oxygen (FiO₂) $\leq 300\text{mmHg}$ ($1\text{mmHg}=0.133\text{kPa}$), or significant progress in chest CT findings of pneumonia within 24-48 hours $\geq 50\%$. Critical cases are defined as those who are admitted to the intensive care unit for mechanical ventilation or had a FiO₂ of at least 60% or more^{21,22}. Finally, fifty-one

patients were included with demographics and clinical characteristics recorded. The flowchart of patient selection is shown in Figure 1.

CT protocol

All examinations represented the initial CT scans for every individual patient. All CT images were acquired at the end of inhalation using a 256-row CT scanner (Revolution CT, GE Healthcare, Waukesha, Wisconsin, USA) with detector configuration of 256×0.625 mm or using a 192-slice CT scanner (Somatom Force, Siemens Healthineers, Forchheim, Germany) with detector collimation of 192×0.6 mm. Other acquisition parameters for these two scanners were set as follows: tube voltage of 120 kV, automatic tube current modulation of 100-300 mA (AutomA, GE Healthcare; CareDose 4D, Siemens Healthineers), pitch of 0.99-1.375 and matrix of 512×512 .

Images were reconstructed at slice thickness/interval of 1-1.25 mm with a hybrid adaptive statistical iterative reconstruction (40% level) using standard (mediastinal) and bone plus (lung) kernels (GE Healthcare) or with an advanced modeled iterative reconstruction (strength 3) using Br40 (mediastinal) and BI57 (lung) kernels (Siemens Healthineers). The mediastinal and lung window width and level were set as 350/40HU and 1500/-700HU (GE Healthcare) or 400/40HU and 1500/-500 (Siemens Healthineers) respectively to evaluate the abnormalities in the mediastinum and lung parenchyma.

Qualitative image analyses

All the chest CT images were analyzed by two radiologists (Blinded [a senior thoracic radiologist with more than 30 years' experience] and Blinded [a thoracic radiologist with 8

years' experience]) without access to clinical or laboratory findings. According to previously published papers for COVID-19^{6-8,23}, the CT image findings of ground-glass opacity (GGO), consolidation, crazy-paving pattern, septal thickening and pulmonary fibrosis were included in calculating the severity score of each lobe, which was classified from score 0 to score 4 with an increment of 1, representing a degree of involvement of 0 to $\geq 75\%$ with an increment of 25%, respectively²⁴. Total severity scores for the whole lung was the sum of five lung lobe scores (0-20 scores).

Since previous reports^{24,25} showed that the main CT manifestations of COVID-19 pneumonia at baseline were bilateral, peripheral and basal GGO and consolidation, and developed into crazy-paving and consolidation with multi-lobar involvement at the peak of lung involvement, we took the sum extent of crazy-paving and consolidation involving the lung as an index to evaluate the progression of pneumonia. Crazy-paving pattern is defined as consisting of scattered or diffuse ground-glass attenuation with superimposed interlobular septal thickening and intralobular lines²⁶ while consolidation is defined as a uniform increase of lung parenchyma with obscuration of the underlying vessels⁵. The sum involvement of crazy-paving and consolidation of each lobe was scored using the above-mentioned scoring criteria, and the sum of the five lobes was taken as the total lung scores(0-20 scores)²⁴.

Quantitative image analyses

All the reconstructed images were transferred to the workstation for pulmonary quantitative analyses using CT Pulmo 3D software (CT Pulmo3D-Syngo.via VB20, Siemens Healthineers). After loading the CT data, an automatic segmentation mode of lung parenchyma (left and right lung mode) was applied and then manual adjustment if necessary was made to

ensure accurate lung segmentation. For the segmented lung, the volume(ml), relative volume(%), mean lung density(MLD)(HU) and full width at half maximum(FWHM)(HU) were measured within the preset threshold range of -950HU and -200HU. The setting of the threshold range is based on the findings that CT values of normal parenchyma range from -950HU to- 750HU while those in vessels or pneumonia are \geq -200HU, from the instructions of the manufacturer, previous studies²⁷⁻²⁹, and our practical experience. The evaluation index method was displayed by quantifying the percentage of the voxel below the low attenuation value (LAV) (threshold of -950HU) and above the high attenuation value (HAV) (threshold of -200 HU). The FWHM parameter marks the width of frequency distribution at half of the maximum CT value, representing the heterogeneity of lung tissue density³⁰.

A subrange analysis method was used to display the relative volume of the segmented lung within a predetermined HU range, which was -1000 to -200HU (in 8 colors representing 8 subranges). Percentile analysis was used to calculate and display relative volume (HU) within predefined percentage values of the lung segmentation(0-100%), representing the cumulative number of voxels. Considering that the threshold of GGO has been reported to range from -800 to -500 HU³¹, the threshold range of normal CT values in our study was finally set at between -950HU and -800HU instead of -950 to -750 HU to assess the relative volume of residual normal lung density of COVID-19 pneumonia.

In order to facilitate readers to better understand the performance of lung quantitative analysis methods on pneumonia, we included normal lung CT images from another 10 cases collected retrospectively for the comparison.

Statistical analyses

Analyses were done with SPSS software version 16.0 and MedCalc software (version 15.2.2, MedCalc Software) with P -value < 0.05 indicating a statistical difference. Continuous variables were presented as mean and standard deviations(SD) if normally distributed, and as median and interquartile range (IQR) values if non-normally distributed, while categorical variables were described as frequency rates and percentages. The normality of continuous variables was tested for using Shapiro-Wilk tests. Comparisons among the groups were performed using Fisher's exact test (for categorical data), one-way ANOVA or the Kruskal-Wallis H test (for continuous data). Using clinical stages as the reference standard, the sensitivity, specificity, accuracy and the associated area under the receiver operating characteristic curve (AUC) with 95% confidence interval (CI) of qualitative and quantitative indicators were calculated.

Results

Patient characteristics

The demographics and clinical characteristics of all patients are summarised in the Table 1. In the full cohort, the mean age was 54 years ± 17 (range 25–94), with no gender difference (29 [57%] men and 22 [43%] women). The most common symptoms at symptom onset were fever (50 [98%] patients) and dry cough (22 [43%]), with 17 (33%) patients had underlying diseases. Twenty patients (39%) suffered from acute respiratory distress syndrome (ARDS), of which 13 were transferred from other hospitals (six in group B and seven in group C). Patients in group C were much older (58 years ± 27) than group A (36 years ± 10) ($p=0.036$), and had more

cases of underlying diseases(12[50%]) and ARDS (13[54%]) than groups A and B (A, 1[8%] and none; B, 4[26%] and 6[40%], respectively) ($p < 0.05$).

Qualitative indicators

Comparisons of the qualitative image findings among the three groups are shown in Table 2. In the full cohort, the common patterns seen on chest CT were bilateral and peripheral GGO (44[86%]), consolidation (43[84%]), crazy-paving pattern (37[73%]), septal thickening (36[71%]) and air bronchogram (32[63%]). No significant differences in GGO were found among the three groups. Patients in group C had more CT manifestations of consolidations(22[92%]), crazy-paving pattern(20[83%]), air bronchogram(20[83%]), septal thickening(18[75%]) and pleural effusion (8[33%]) than those in group A(7[58%], 6[50%], 3[25%], 7[58%], none, respectively) (All $p < 0.05$), but were similar to group B. Pulmonary fibrosis, as an uncommon CT finding, accounts for similar frequencies in the three groups. From group A to groups B and C, in more severe cases, the number of involved lung segments and lobes, the total severity score for the whole lung and total score for crazy-paving and consolidation all increased, significantly higher in groups B and C(All $p < 0.05$). And the frequencies of these image patterns were similar between group B and group C. The time interval between the initial CT scan and the symptom onset were longer in groups B and C (8 days[IQR,4,13], 10 days[6,14]) than that in group A(4 days[1,7])(both $p < 0.05$), but was similar between group B and group C.

Quantitative indicators

Comparisons of quantitative analyses and image examples are shown in Table 3 and Figure 2. A normal lung CT group (n = 10) was included for the quantitative comparison with the other three COVID-19 pneumonia groups. Patients in group C had significantly lower total lung volumes, higher MLD, higher FWHM and higher HAV than the other three groups (All $p < 0.001$), but showed similar LAV values to them. No statistical differences in the quantitative indicators were found between groups A and B except MLD, which was higher in group B than group A ($P = 0.038$). The percentile analysis showed that relative volume of normal lung density (from -950HU to -800HU) within the total segmented lung was 43.01% (SD, 13.42) in group C, which was significantly lower than those in the other three groups (group A 87.83% [SD, 6.73]; group B 62.25% [SD, 14.80]; normal group 88.91% [SD, 3.35]) (All $p < 0.001$) (Fig 3). Compared with the normal group, the relative volume of normal lung density was lower in group B ($P < 0.001$) but was similar to group A, with the latter two groups significantly different from each other ($p = 0.03$).

Identification of different clinical stages with CT indicators

By using the receiver operating characteristic curves, the threshold values of statistically significant parameters were determined to optimize both the sensitivity and the specificity for differentiating each group from the other two groups (Table 4)

For example, patients in groups C were significantly different from groups A and B with a higher number of involved lung segments (> 8 , sensitivity and specificity of 100% and 37%), higher total severity score (> 10 , 67% and 74%), higher total score for crazy-paving and consolidation (> 4 , 87% and 44%), higher MLD (> -779 HU, 100%, and 85%), higher

FWHM(>116HU,83% and 81%), and lower relative volume of normal lung density ($\leq 50\%$, 83% and 92%).

As the intermediate stage between group A and group C, group B was similar to these two groups in qualitative indicators except for the total score for crazy-paving and consolidation which is significantly different from group A (threshold value of 8, sensitivity and specificity of 92% and 40%). Compared with group B, group C showed higher MLD(>779HU, sensitivity and specificity of 100% and 73%) and FWHM(>128HU,75% and 80%) but lower relative volume of normal lung density ($\leq 50\%$, 83% and 80%), while group A showed lower MLD(≤ 816 HU,92% and 80%) and FWHM (≤ 102 HU, 92% and 67%) but higher relative volume of normal lung density (>80%, 92% and 100%)(Table 5).

In short, using qualitative indicators could not differentiate group C from group B, but quantitative indicators could distinguish them. Based on the results of qualitative and quantitative indicators to distinguish the three groups, a summary diagram was drawn with the illustrations attached for each group (Figure 4).

Combined use of the qualitative and quantitative indicators showed higher sensitivity(90%), specificity(100%) and accuracy (92%) in distinguishing groups B and C from group A than qualitative indicators alone (sensitivity, specificity and accuracy: 69%, 83% and 73%, $p < 0.001$) (Table 6). Based on the qualitative results of distinguishing groups B and C from group A, we further achieved sensitivity of 92% , specificity of 87% , and accuracy of 90% to distinguish group C from group B using the quantitative indicators(Figure 5).

Discussion

The novel coronavirus SARS-CoV-2, the seventh member of the coronaviridae family, leads to a very high case-fatality rate of COVID-19, varying by country, age and the presence of underlying disease²⁻⁴. It's difficult to obtain the exact mortality at present as the COVID-19 is still spreading across the world and posing a significant global health threat because of its high infectiousness and lack of specialized treatments. Since the mainstay of treatment for COVID-19 pneumonia has been supportive care, early identification of clinical stages is essential for initial management, especially for critical patients, who are related to high mortality⁴ and need aggressive treatments and intensive care treatment.

Similar to previous studies^{1,4}, the predisposing conditions for COVID-19 pneumonia in the critical cases tended to be old age(>55 years old) and original existing disease(such as chronic pulmonary disease, cardiovascular disease and cerebrovascular disease), perhaps due to their poor immunity. The predominant abnormal chest CT pattern observed was bilateral and peripheral GGO and consolidation^{6,23}, the frequency of the former was not specific in identifying the cases in different clinical stages. This can be explained by the pathological findings that early alveolar damage caused by virus invasion into pulmonary interstitium includes alveolar edema, protein exudate and thickening of the interlobular interstitium^{32,33} which will evolve to diffuse alveolar damage with cellular fibromyxoid exudate as the disease progresses to the critical stage³⁴, both manifesting as GGO. From the ordinary stage to the severe/critical stage, in more severe cases, the number of involved lung segments and lobes, the frequencies of consolidation, crazy-paving pattern and air bronchogram all increased, making the total severity score for the whole lung and total score for crazy-paving and consolidation significantly higher in the severe/critical cases compared to the ordinary cases. These findings were consistent with

previous studies^{16,23} showing that the progression of septal thickening, crazy-paving and lung consolidation were noted in the progression or peak period of pneumonia(1-3 weeks). Progression of consolidation and crazy-paving might represent further infiltration of the lung parenchyma and lung interstitium^{5,35}, indicating that the virus has invaded the respiratory epithelium which is characterized by diffuse alveolar damage and necrotizing bronchitis, leading to alveoli completely filled by inflammatory exudation. Some of the severe(2[13%]) and critical cases(8[33%]) in our study presented with pleural effusion on CT, the presence of which has been shown as a poor prognostic indicator in patients with Middle East respiratory syndrome coronavirus³⁶. One of our critical cases with bilateral pleural effusion was found dead during our later follow-up. The time interval between the initial CT scan and the symptom onset in the severe/critical cases were longer than that in the ordinary cases, partly might be due to the late initial CT scan for the transferred patients(33%[13/39]) from the county or township hospitals with limited medical equipment and ability, and partly due to the fact that some cases were not hospitalized until their clinical symptoms progressed.

The COVID-19 viral disease is now officially a pandemic, the World Health Organization announced Mar 10th, 2020. Chest CT has been widely used as an effective tool for diagnosing patients with COVID-19 pneumonia. However, the diversified CT patterns of COVID-19 pneumonia made it difficult to accurately and quickly assess the clinical severity. Our study demonstrated that severe/critical cases could be distinguished from ordinary cases using the combined qualitative indicators including total severity score for the whole lung and total score for crazy-paving and consolidation (sensitivity, specificity and accuracy: 69%, 83% and 73%). However, the diversity of virus manifestations and small imaging differences between

the critical cases and severe cases make the qualitative indicators insufficient to distinguish them. This shortcoming might be compensated by the quantitative indicators.

Compared with severe cases, critical cases showed higher MLD (>-779 HU, sensitivity and specificity of 100% and 73%) and FWHM (>128 HU, 75% and 80%) but lower relative volume of normal lung density ($\leq 50\%$, 83% and 80%). The combined quantitative indicators could achieve high sensitivity (92%), specificity (87%) and accuracy (90%) in distinguishing critical cases from severe cases, based on the qualitative results of distinguishing severe/critical cases from ordinary cases. Lung density on CT, positively correlated with the proportion of consolidation¹⁶, might mirror an inflammatory response in the lung²⁸. FWHM represents the heterogeneity and density distribution of the lung parenchyma, the higher values of which might indicate mixed and diverse inflammatory components. The residual relative volume of normal lung density might be related to the lung function³⁷. In our critical cases, eight patients with residual normal lung density smaller than 40% received mechanical ventilation for supportive treatment, two of them had died. The substantial difference in the relative volume of residual normal lung density among the three groups, indicating the value is associated with the severity of illness and thus prognosis. The similar LAV values of the three COVID-19 pneumonia groups to the normal CT groups indicated that no obvious sign of emphysema observed in pneumonia at the initial CT scan, as the setting of the LAV threshold for emphysema was -950 HU³⁰. The HAV values increased in more severe cases, indicating an increase in high-density lesions and providing evidence that the total score for crazy-paving and consolidation could be as a qualitative indicator for evaluating disease progression. The higher HAV values (above than -200 HU) in the critical cases also helped explain why the total lung volume within the preset threshold range of -950 HU and -200 HU lower than the ordinary/severe cases.

It should be noted that the time interval between the initial CT scan and the symptom onset ranged from 0 to 20 days in our study, and 63%(32/51) of CT scans weren't obtained at an early stage(0-5 days)^{8,9}. The evolution of diverse CT imaging findings of COVID-19 pneumonia with time⁸ and the interobserver variability of imaging assessment would make the visually accurate evaluation or staging of the disease difficult. However, the method of quantitative analysis of pneumonia based on the lung density and volume changes was standard, except for the manual adjustment if necessary to ensure the accuracy of automatic lung segmentation using the software, which would make it easier and objective for radiologists to evaluate the extent of disease. Different from previous quantitative studies^{14,16,18} which evaluated the extent of the disease by quantifying the CT lung opacification percentage using a deep-learning, computer or computation-based method, our study assessed the extent of pulmonary changes and the severity of COVID-19 by quantifying the relative volume of normal lung density using a commercial CT Pulmo 3D software, which would provide valuable knowledge and a feasible clinical tool for the management of these patients and broaden the technical spectrum of lung quantitative analysis.

Our study had several limitations. First, only 51 patients were included in our study. We hope that the significant findings presented here will encourage a larger cohort study in the future. Second, the application of CT quantification using specific software limits its widespread clinical application. However, the use of qualitative indicators in distinguishing severe/critical cases from ordinary cases would also provide help for initial management for clinical care. Third, only the initial CT scan was included for analysis, more follow-up time points would be assessed in our next research. Fourth, the correlation of clinical features and outcome with the CT features, especially for the quantitative indicators, has not been assessed in our study, this work is currently in progress.

In conclusion, depending on the severity of the disease, the number of involved lung segments and lobes, the frequencies of consolidation, crazy-paving pattern and air bronchogram increased in more severe cases. Using qualitative indicators alone could distinguish severe/critical cases from ordinary cases, but provide little help to differentiate severe cases from critical cases. The combined use of qualitative and quantitative indicators could distinguish cases at different clinical stages, might provide help to facilitate the fast identification and management of critical cases, thus reducing the mortality rate. Critical cases had higher total severity score(>10) and total score for crazy-paving and consolidation(>4) than ordinary cases, and had higher mean lung density(>-779HU) and full width at half maximum(>128HU) but lower relative volume of normal lung density($\leq 50\%$) than ordinary/severe cases. CT imaging findings could help to continuously monitor the treatment effects objectively in the follow-up as well as provide guidance for clinical management and treatment.

Acknowledgments

The study was supported by Overseas Research Project of Science and Technology Talent of Henan Health and Family Planning Commission (Grant No. 2018134 to P. J. L.) .

ACCEPTED

REFERENCES

1. Li K, Wu J, Wu F, et al. The Clinical and Chest CT Features Associated with Severe and Critical COVID-19 Pneumonia. *Invest Radiol.* 2020. Doi: 10.1097/RLI.0000000000000672.
2. CDC COVID-19 Response Team. Severe Outcomes Among Patients with Coronavirus Disease 2019 (COVID-19) - United States, February 12-March 16, 2020. *MMWR Morb Mortal Wkly Rep.* 2020;69:343-346.
3. Onder G, Rezza G, Brusaferro S. Case-Fatality Rate and Characteristics of Patients Dying in Relation to COVID-19 in Italy. *JAMA.* Doi: 2020.10.1001/jama.2020.4683
4. Yang X, Yu Y, Xu J, et al. Clinical course and outcomes of critically ill patients with SARS-CoV-2 pneumonia in Wuhan, China: a single-centered, retrospective, observational study. *Lancet Respir Med.* 2020. DOI:https://doi.org/10.1016/S2213-2600(20)30079-5
5. Zhou S, Wang Y, Zhu T, Xia L. CT Features of Coronavirus Disease 2019 (COVID-19) Pneumonia in 62 Patients in Wuhan, China. *AJR Am J Roentgenol.* 2020 : 1-8.
6. Xiong Y, Sun D, Liu Y, et al. Clinical and High-Resolution CT Features of the COVID-19 Infection: Comparison of the Initial and Follow-up Changes. *Invest Radiol.* 2020. Doi: 10.1097/RLI.0000000000000674.
7. Kanne JP. Chest CT Findings in 2019 Novel Coronavirus (2019-nCoV) Infections from Wuhan, China: Key Points for the Radiologist. *Radiology.* 2020 : 200241. Doi:10.1148/radiol.2020200241

8. Wang Y, Dong C, Hu Y, et al. Temporal Changes of CT Findings in 90 Patients with COVID-19 Pneumonia: A Longitudinal Study. *Radiology* 2020;200843. Doi:10.1148/radiol.2020200843
9. Pan F, Ye T, Sun P, et al. Time Course of Lung Changes On Chest CT During Recovery From 2019 Novel Coronavirus (COVID-19) Pneumonia. *Radiology*. 2020;200370. <https://doi.org/10.1148/radiol.2020200370>
10. Wu J, Wu X, Zeng W, et al. Chest CT Findings in Patients with Corona Virus Disease 2019 and its Relationship with Clinical Features. *Invest Radiol*. 2020. Doi:10.1097/RLI.0000000000000670
11. Ufuk F. 3D CT of Novel Coronavirus (COVID-19) Pneumonia. *Radiology*. 2020;201183. Doi:10.1148/radiol.2020201183
12. Huang P, Liu T, Huang L, et al. Use of Chest CT in Combination with Negative RT-PCR Assay for the 2019 Novel Coronavirus but High Clinical Suspicion. *Radiology*. 2020;295:22-23. Doi:10.1148/radiol.2020200330
13. Qi X, Lei J, Yu Q, et al. CT imaging of coronavirus disease 2019 (COVID-19): from the qualitative to quantitative. *Annals of Translational Medicine*; Vol 8, No 5 (March 2020): *Annals of Translational Medicine*. 20202020.doi: 10.21037/atm.2020.02.91
14. Hyewon Choi, Xiaolong Qi, Soon Ho Yoon, et al. Extension of Coronavirus Disease 2019 (COVID-19) on Chest CT and Implications for Chest Radiograph Interpretation. *Radiology: Cardiothoracic Imaging*. 2020 2:2 <https://doi.org/10.1148/ryct.2020200107>

15. Ran Yang, Xiang Li, Huan Liu, et al. Chest CT Severity Score: An Imaging Tool for Assessing Severe COVID-19 *Radiology: Cardiothoracic Imaging*. 2020 2:2. <https://doi.org/10.1148/ryct.2020200047>
16. Cong Shen, Nan Yu, Shubo Cai, et al. Quantitative computed tomography analysis for stratifying the severity of Coronavirus Disease 2019. *Journal of Pharmaceutical Analysis*, 2020. <https://doi.org/10.1016/j.jpha.2020.03.004>.
17. Li K, Fang Y, Li W, et al. CT image visual quantitative evaluation and clinical classification of coronavirus disease (COVID-19). *Eur Radiol*. 2020. Doi:10.1007/s00330-020-06817-6
18. Lu Huang, Rui Han, Tao Ai, et al. Serial Quantitative Chest CT Assessment of COVID-19: Deep-Learning Approach. *Radiology: Cardiothoracic Imaging*. 2020 2:2. <https://doi.org/10.1148/ryct.2020200075>
19. Zu ZY, Jiang MD, Xu PP, et al. Coronavirus Disease 2019 (COVID-19): A Perspective from China. *Radiology* 2020:200490. Doi:10.1148/radiol.2020200490
20. WHO. Clinical management of severe acute respiratory infection when novel coronavirus (nCoV) infection is suspected. Jan 11, 2020. [https://www.who.int/publications-detail/clinical-management-of-severe-acute-respiratory-infection-when-novel-coronavirus-\(ncov\)-infection-is-suspected](https://www.who.int/publications-detail/clinical-management-of-severe-acute-respiratory-infection-when-novel-coronavirus-(ncov)-infection-is-suspected) (accessed Feb 8, 2020).
21. Vandroux D, Allyn J, Ferdynus C, et al. Mortality of critically ill patients with severe influenza starting four years after the 2009 pandemic. *Infect Dis (Lond)*. 2019. 51(11-12): 831-837.
22. Domínguez-Cherit G, Lapinsky SE, Macias AE, et al. Critically Ill patients with 2009 influenza A(H1N1) in Mexico. *JAMA*. 2009. 302(17): 1880-1887.

23. Shi H, Han X, Jiang N, et al. Radiological findings from 81 patients with COVID-19 pneumonia in Wuhan, China: a descriptive study. *Lancet Infect Dis.* 2020 .Doi: 10.1016/S1473-3099(20)30086-4
24. Bernheim A, Mei X, Huang M, et al. Chest CT Findings in Coronavirus Disease-19 (COVID-19): Relationship to Duration of Infection. *Radiology.* 2020;200463.Doi:10.1148/radiol.2020200463
25. Kanne JP, Little BP, Chung JH, et al. Essentials for Radiologists on COVID-19: An Update-Radiology Scientific Expert Panel. *Radiology.* 2020;200527.Doi:10.1148/radiol.2020200527
26. Rossi SE, Erasmus JJ, Volpacchio M, Franquet T, Castiglioni T, McAdams HP. "Crazy-paving" pattern at thin-section CT of the lungs: radiologic-pathologic overview. *Radiographics.* 2003. 23(6): 1509-1519.
27. Zach JA, Newell JD Jr, Schroeder J, et al. Quantitative computed tomography of the lungs and airways in healthy nonsmoking adults. *Invest Radiol.* 2012. 47(10): 596-602.
28. Karimi R, Tornling G, Forsslund H, et al. Lung density on high resolution computer tomography (HRCT) reflects degree of inflammation in smokers. *Respir Res.* 2014. 15: 23.
29. Cheng T, Li Y, Pang S, et al. Normal lung attenuation distribution and lung volume on computed tomography in a Chinese population. *Int J Chron Obstruct Pulmon Dis.* 2019. 14: 1657-1668.
30. Gawlitza J, Sturm T, Spohrer K, et al. Predicting Pulmonary Function Testing from Quantified Computed Tomography Using Machine Learning Algorithms in Patients with COPD. *Diagnostics (Basel).* 2019. 9(1).

31. Yabuuchi H, Matsuo Y, Tsukamoto H, et al. Evaluation of the extent of ground-glass opacity on high-resolution CT in patients with interstitial pneumonia associated with systemic sclerosis: comparison between quantitative and qualitative analysis. *Clin Radiol* 2014;69(7):758-764.
32. Tian S, Hu W, Niu L, Liu H, Xu H, Xiao SY. Pulmonary Pathology of Early Phase SARS-COV-2 Pneumonia. *J Thorac Oncol*. 2020. Doi: 10.1016/j.jtho.2020.02.010.
33. Franquet T. Imaging of pulmonary viral pneumonia. *Radiology*. 2011. 260(1): 18-39.
34. Xu Z, Shi L, Wang Y, et al. Pathological findings of COVID-19 associated with acute respiratory distress syndrome. *Lancet Respir Med*. 2020 .Doi: 10.1016/S2213-2600(20)30076-X
35. Koo HJ, Lim S, Choe J, Choi SH, Sung H, Do KH. Radiographic and CT Features of Viral Pneumonia. *Radiographics*. 2018. 38(3): 719-739.
36. Das KM, Lee EY, Enani MA, et al. CT correlation with outcomes in 15 patients with acute Middle East respiratory syndrome coronavirus. *AJR Am J Roentgenol*. 2015. 204(4): 736-42.
37. Tanaka R, Tani T, Nitta N, et al. Pulmonary Function Diagnosis Based on Respiratory Changes in Lung Density With Dynamic Flat-Panel Detector Imaging: An Animal-Based Study. *Invest Radiol*. 2018;53:417-423.

Figure 1. Flowchart of patient selection. COVID-19=coronavirus disease 2019

Figure 2. Chest CT images and related quantitative analysis images of a 23-year-old man in the normal group, a 36-year-old woman in group A, a 48-year-old man in group B and a 66-year-old man in group C. From group A to group C, depending on the severity of the disease, the number of involved lung segments (1,7,19), the total severity score (2,7,16) and the total score for crazy-paving and consolidation increased in more severe cases (1,5,12). Three-dimensional volume-rendering(VR) images showed the distribution of lesions in the lung clearly while the subrange images displayed the distribution of lesions by using different colors representing different subranges of HU ranges, such as red color representing higher lung density of consolidation. The percentile curve images manifested that the relative volume area of normal CT density (-950HU to -800HU) under the curve gradually decreased from the normal group, group A to group C.

Figure 3. The average relative volume of normal lung density (from -950HU to -800HU) within the total segmented lung was 88% in group A, 62% in group B and 43% in group C respectively (A). Examples of chest CT coronal images and three-dimensional volume-rendering(3D-VR) images showed that a 28-year-old man in group A had the peripheral distribution of multiple focal consolidations and ground-glass opacities(GGO) in bilateral lungs, with residual normal lung density of 90% based on the percentile analysis; a 48-year-old woman in group B had multiple patchy consolidations, GGO, and crazy-paving sign, with residual normal lung density of 70%; a 58-year-old man in group C had diffuse consolidation, crazy-paving, and air bronchogram, with residual normal lung density of 20% (B). 3D-VR images clearly showed the distribution of lesions in the lung with the form of high density.

Figure 4. A summary diagram of identifying ordinary, severe and critical cases using the qualitative and quantitative indicators. Each stage is attached to two axial CT images from two separate patients. Rel.vol=relative volume; MLD=mean lung density; FWNH=full width at half maximum.

Figure 5. Axial chest CT images and percentile curve images from critical and severe cases. The upper left severe case and the upper right severe case had the same residual normal lung density of 60% based on the percentile analysis, but displayed different image manifestations and distribution patterns, with the MLD and FWHM of -746HU and 89HU respectively in the former, and -728 HU and 104 HU respectively in the latter. Both the upper right severe case and the lower middle critical case had the diffuse distribution of crazy-paving and consolidation, but the latter had higher MLD (-677HU) and FWHM(167HU), and lower residual normal lung density(40%) than the former. The critical case suffered from acute respiratory distress syndrome and received mechanical ventilation for support. MLD=mean lung density; FWNH=full width at half maximum.

Figure 1

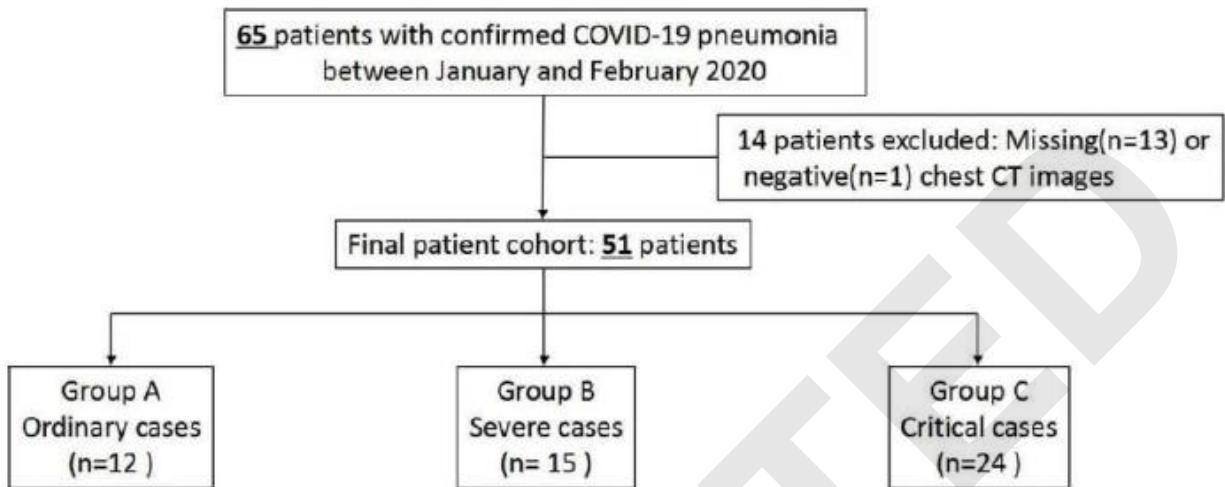


Figure 2

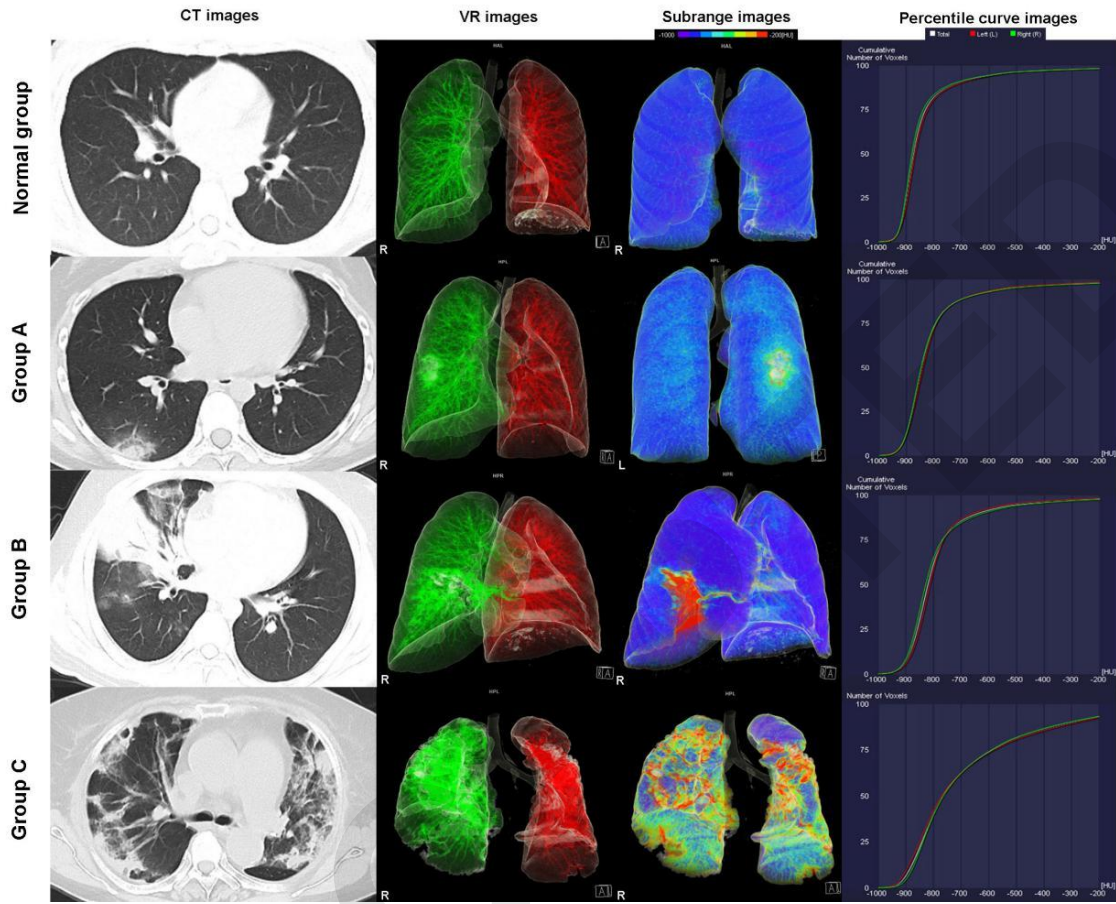


Figure 3

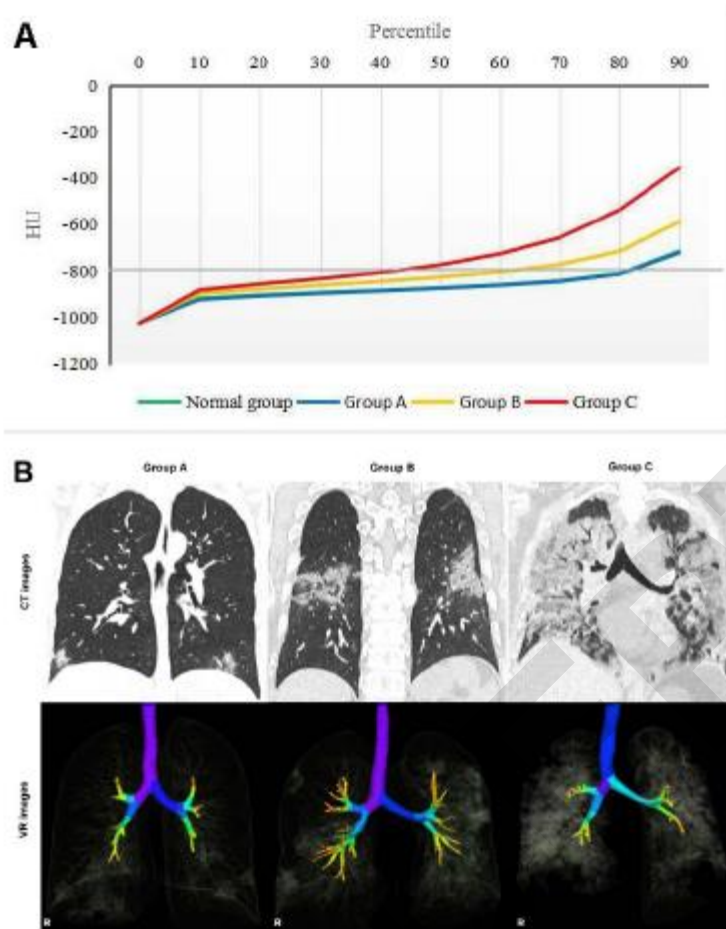


Figure 4

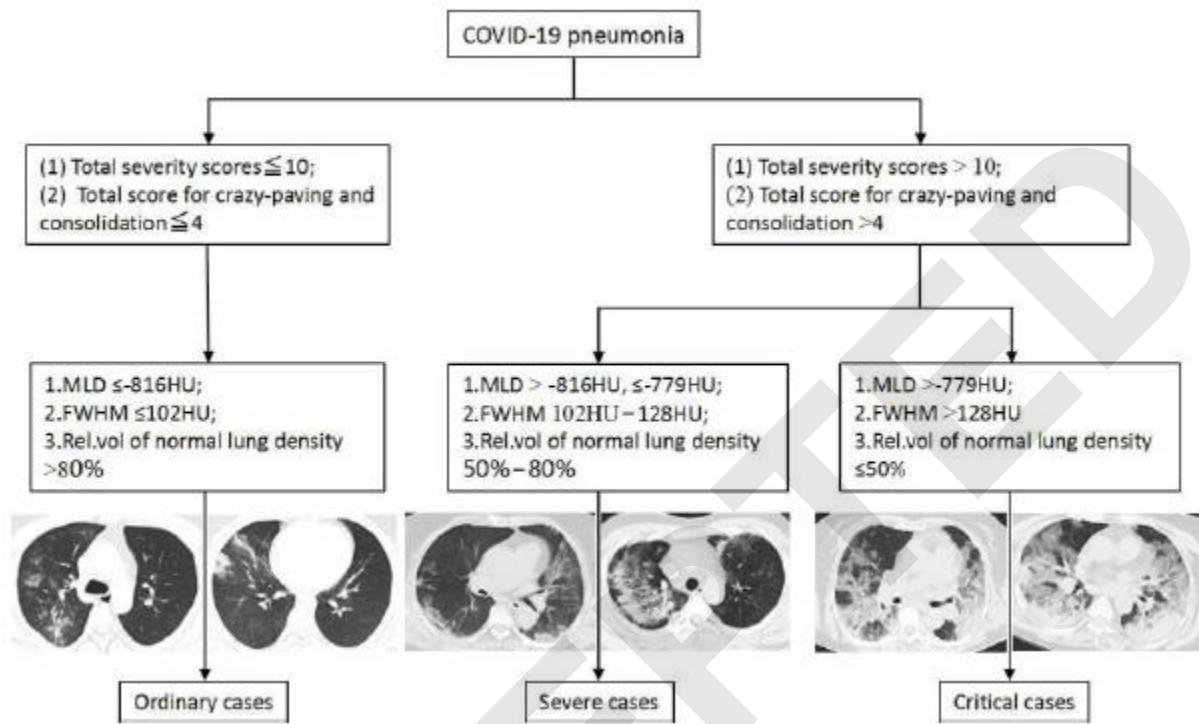


Figure 5

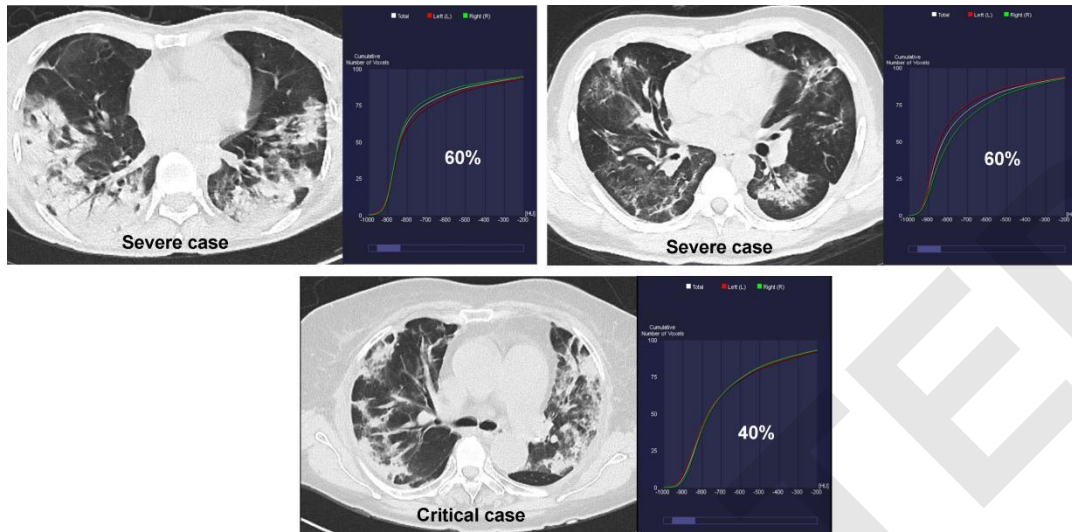


Table 1 Demographics and clinical characteristics of patients with COVID-19 pneumonia

Parameter	All patients (n=51)	Group A (n=12)	Group B (n=15)	Group C (n=24)	p value†
Sex(M/F)	29/22	7/5	8/7	14/10	0.948
*Age(y)	54±17	36±10	47±14	58±27	0.046
Exposure history	43(84 %)	12(100%)	13(87%)	18(75%)	0.872
Initial signs and symptoms of onset					0.764
Fever	50(98%)	11(92%)	15(100%)	24(100%)	
Dyspnea	12(24%)	1(8%)	4(27%)	7(29%)	
Fatigue	16(31%)	5(42%)	5(33%)	6(25%)	
Dry cough	22(43%)	2(17%)	8(53%)	12(50%)	
Underlying disease	17(33%)				0.002
Chronic pulmonary disease	3(6 %)	0	0	3(13%)	
Cardiovascular disease	8(16%)	0	2(13%)	6(25%)	
Cerebrovascular disease	5(10%)	0	2(13%)	3(13%)	
Malignant tumor	1(2%)	1(8%)	0	0	
Comorbidities					
Acute respiratory distress syndrome	20(39%)	0	6(40%)	13(54%)	0.032
Treatment					
High flow nasal cannula	25(49%)	2(17%)	6(40%)	17(71%)	<0.001
Mechanical ventilation	7(14%)	0	0	8(33%)	0.310
ICU admission	23(45%)	0	7(47%)	16(67%)	<0.001

Note: Data are the numbers with the percentage in parentheses except where specified.* Data are mean ± standard deviation. †Difference among groups A-C.

Exposure history indicates the history of cases exposed to infected individuals or epidemic areas.

Table 2 Comparison of CT image findings among different groups

Parameter	Group A (n=12)	Group B (n=15)	Group C (n=24)	p value†
Unilateral/Bilateral	8(67%)/4(33%)	2(13%)/13(87%)	0/24(100%)	<0.001
Number of involved segments*	9(3,13)	14(7,18)	17(12,18)	0.018
Involved lobes				
0-2/3-5	8(67%)/4(33%)	3(20%)/12(80%)	0/24(100%)	<0.001
Total severity score*	6(2,9)	9(4-14)	12(9,17)	<0.001
Total score for crazy-paving and consolidation*	4(2,7)	8(5,12)	9(6,14)	<0.001
Lesion distribution				0.040
Peripheral	8(67%)	9(60%)	13(54%)	
Random	4(33%)	4(27%)	4(17%)	
Diffuse	0	2(13%)	7(29%)	
Ground-glass opacity	8(67%)	13(87%)	23(96%)	0.097
Consolidation	7(58%)	14(93%)	22(92%)	0.002
Crazy-paving pattern	6(50%)	11(73%)	20(83%)	0.001
Air bronchogram	3(25%)	9(75%)	20(83%)	<0.001
Septal thickening	7(58%)	11(73%)	18(75%)	0.210
Pulmonary fibrosis	1(8%)	6(40%)	6(25%)	0.549
Pleural effusion	0	2(13%)	8(33%)	0.019
From onset of symptoms to CT scan (d)*	4(1,7)	8(4,13)	10(6,14)	0.007

Note: Data are the numbers with the percentage in parentheses except where specified.* Data are median (interquartile range). †Difference among groups A-C.

Table 3 Comparison of quantitative indicators among the normal group and three COVID-19 pneumonia groups

Groups	Volume [mL]	MLD [HU]	FWHM [HU]	LAV [%]	HAV [%]
Normal group (n=10)	4850 (761)	-863.91 (45.7)	73.00 (9.01)	1.57 (0.56)	1.49 (0.24)
Group A (n=12)	4651 (1000)	-833.82 (16.41)	81.90 (16.12)	2.07 (1.80)	1.53 (0.24)
Group B (n=15)	3884 (913)	-775.70 (58.31)	112.30 (45.47)	1.68 (0.87)	2.44 (1.55)
Group C (n=24)	2231 (639)	-691.71 (54.18)	140.80 (36.09)	0.74 (0.63)	5.71 (1.98)
<i>P</i> value †	<.001	<.001	<.001	.053	<.001

Note: Data are expressed as means(standard deviation). †Difference among normal groups, groups A-C.

The threshold for the lung volume calculation was set ranging from -950HU to -200HU. Rel.vol=relative volume; MLD=mean lung density; FWHM=full width at half maximum; LAV=low attenuation value; HAV=high attenuation value.

Table 4 Thresholds, sensitivities, and specificities for distinguishing each group from the other two groups

Parameter	A (positive, n=12) vs. B+C (negative, n=39)				C (positive, n=24) vs. A+B (negative, n=27)			
	AUC [95%CI]	Threshold value	Sensitivity (%)	Specificity (%)	AUC [95%CI]	Threshold value	Sensitivity (%)	Specificity (%)
Number of involved segments	NS	NS	NS	NS	0.71 [0.56,0.85]	>8*	100(24)	37(10)
Total severity score	0.72 [0.58,0.86]	≤10*	83(10)	51(20)	0.75 [0.60,0.89]	>10*	67(16)	74(20)
Total score for crazy-paving and consolidation	0.75 [0.61,0.89]	≤4**	58(7)	80(31)	0.66 [0.51,0.82]	>4**	87(21)	44(12)
MLD[HU]	0.96 [0.82,0.98]	≤-816**	91(11)	90(35)	0.94 [0.80,0.99]	>-779**	100(24)	85(23)
FWHM[HU]	0.87 [0.70,0.96]	≤102**	91(11)	77(30)	0.86 [0.70,0.96]	>116**	83(20)	81(22)
Rel.vol of normal lung density (%)	0.93 [0.86,1.00]	>80**	91(11)	100(39)	0.94 [0.80,0.99]	≤50**	83(20)	92(25)

Note: Rel.vol=relative volume; MLD=mean lung density; FWHM=full width at half maximum; NS=no statistical difference.

* p <0.05, or ** p <0.01 indicates the difference between each group and the other two groups. No significant different differences were found between the cases of group B and the cases of groups A and C.

Data in parentheses are numbers of corrected diagnoses used to calculate percentages.

Sensitivity values are numbers of positive cases used to calculate percentages.

Specificity values are numbers of negative cases used to calculate percentages

Number of groups A, B and C=12,15 and 24 respectively.

Table 5 Thresholds, sensitivities, and specificities for distinguishing group A from group B and group C from group B

Parameter	A(positive, n=12) vs.B (negative,n=15)			C(positive,n=24) vs.B (negative,n=15)		
	Threshold value	Sensitivity (%)	Specificity (%)	Threshold value	Sensitivity (%)	Specificity (%)
Number of involved segments	NS	NS	NS	NS	NS	NS
Total severity score	NS	NS	NS	NS	NS	NS
Total score for crazy-paving and consolidation	≤7**	92(11)	40(6)	NS	NS	NS
MLD[HU]	≤-816**	92(11)	80(12)	>-779**	100(24)	73(11)
FWHM[HU]	≤102**	92(11)	67(10)	>128**	75(18)	80(12)
Rel.vol of normal lung density(%)	>80**	92(11)	100(15)	≤50**	83(20)	80(12)

Note: Rel.vol=relative volume; MLD=mean lung density; FWNH=full width at half maximum; NS=no statistical difference.

**p<0.01 indicates the difference between group A and group B, and group C and group B.

Data in brackets are 95% confidence intervals.

Data in parentheses are numbers of patients used to calculate the percentage.

Sensitivity values are numbers of positive cases used to calculate percentages.

Specificity values are numbers of negative cases used to calculate percentages

Table 6 The performance of combined CT qualitative and quantitative indicators for identifying different groups of COVID-19 pneumonia

Indicators	Groups	AUC [95%CI]	p value	Sensitivity (%)	Specificity (%)	Accuracy (%)
Qualitative	B+C(positive, n=39) vs.A(negative, n=12)	0.87 [0.71,0.96]	0.033	69 (27)	83 (10)	73(37)
Qualitative and quantitative	B+C(positive, n=39) vs.A(negative, n=12)	0.99 [0.88,1.00]	<0.001	90(35)	100(12)	92(47)
	C (positive, n=24) vs. B (negative, n=15)	0.92 [0.73,0.99]	<0.001	92(22)	87(13)	90(35)

Note: Data in parentheses are numbers of patients used to calculate the percentage. Data in brackets are 95% confidence intervals.

Sensitivity values are numbers of positive cases used to calculate percentages.

Specificity values are numbers of negative cases used to calculate percentages